

# SACs phenomena in SiIV regions of 42 BeV stars

E. Lyratzi, E. Danezis, M. Stathopoulou, E. Theodossiou, D. Nikolaidis, C. Drakopoulos & A. Soulikias

University of Athens, School of Physics  
Department of Astrophysics, Astronomy and Mechanics  
Panepistimiopolis, Zografos 157 84  
Athens – Greece

## Abstract

In this paper we present a study of the UV SiIV resonance lines of 42 BeV stars' spectra, using the model proposed by Danezis et al. (2002b, 2003). This model is based on the idea of independent density layers in the regions where the spectral lines that present SACs (DACs) are created. We calculated the apparent rotation ( $V_{\text{rot}}$ ) and expansion/contraction velocities ( $V_{\text{exp}}$ ) of these density regions, as well as their  $\xi$  value, which is an expression of the optical depth. We also present the relation among these parameters and their evolution with the spectral subtype.

**Key words:** early type stars, Be stars, ultraviolet spectra, DACs, SACs, SiIV

## Introduction

The ultraviolet resonance lines of SiIV ( $\lambda\lambda$  1393.755, 1402.77 Å) arise from the transition  $3s^2S-3p^2P^0$ . This doublet is usually an intense feature in the spectra of early type stars and provides us with a useful tool for the study of the stellar atmosphere's structure. Thus, it has been studied by many researchers. It has been proposed that the UV SiIV doublet is a great criterion for the spectral classification (Panek & Savage 1976, Henize et al. 1976, 1981, Walborn & Nichols-Bohlin 1987, Prinja 1990), as well as for the study of mass-loss (Snow & Marlborough 1976, Snow & Morton 1976, Lamers & Snow 1978, Hubeny et al. 1985, 1986) and superionization in the early-type stellar atmospheres (Hubeny et al. 1985, 1986).

The peculiar profile and the asymmetries of the UV SiIV resonance lines has been attributed to blended lines (Hubeny et al. 1985, 1986, Israelian 1995) or to Satellite Absorption Components (SACs), which originate in the circumstellar material, where density regions occur (Underhill 1974, 1975, Snow & Marlborough 1976, Snow 1977, Gathier et al. 1981, Marlborough 1982, Marlborough & Peters 1982, Henrichs et al. 1983, Plavec 1983, Codina et al. 1984, Sahade 1984, Sahade & Brandi 1985, Danezis 1984, 1986, Hutsemekers 1985, Hubeny et al. 1985, 1986, Aydin et al. 1988, Doazan et al. 1988, Bruhweiler et al. 1989, Sapar & Sapar 1992, Kempner & Richards 1999, Danezis et al. 1991, 2002, 2003).

Panek & Savage (1976) in their study of 118 OAO-2 spectra of O and B stars found that the UV SiIV lines' strength depends on the spectral type and luminosity class. In the case of dwarfs, the SiIV feature increases in strength from O type stars, presents a maximum at B0-B1 and disappears when the B3 subtype is reached. Besides, the doublet gets stronger from dwarfs to supergiants.

Henize et al. (1976, 1981) found that the UV SiIV doublet appears stronger in the B0-B2 stars' spectra than in the spectra of the same spectral type stars that present emission. By the time the B3 spectral subtype is reached, the SiIV resonance lines disappear. In the case of luminosity classes I to III, the SiIV lines are very strong and present emission among the O4-B0 supergiants, while their strength decreases and the emission disappears towards B3 supergiants. They considered the lack of SiIV emission in the B1 supergiants as a useful criterion for distinguishing them from earlier supergiants.

Lamers & Snow (1978) found that in the spectra of some B3V stars or later the shifted, circumstellar SiIV lines are present, while the photospheric component is absent. The shifted SiIV component is seen in stars as late as B5V. They also found that Be and shell stars present shifted components of SiIV lines.

Kondo et al. (1981) studied the binary system U Cephei, which consists of a B7V primary and a G8III-IV secondary. They reported variations of the total absorption, perhaps due to hot regions on the B star and gas streaming effects. By comparing with the far-UV spectra of B stars, they found that the SiIV and CIV doublet lines are too strong for a B7 star, while they are comparable to a B0-1 star.

Marlborough (1982) and Marlborough & Peters (1982) observed the UV SiIV doublet in the spectra of B5 stars. They also observed their appearance in stars as cool as B8. They reported variability of the lines' strength, but found no evidence of their total disappearance. Finally, they found that the UV SiIV and CIV lines become fainter by the decrease of  $v_{\text{sin}i}$  and proposed that this may be due to the hot component of the circumstellar envelope not being distributed with spherical symmetry.

Henrichs et al. (1983) studied the UV spectra of the B0.5IVe star  $\gamma$  Cas and observed "narrow absorption components" of the SiIV, CIV and NV ions. They observed strong variations in the shape of these lines, with velocities between -650 and -1500 km/s. They proposed that successive expansion of the matter, which is assumed to be spherical symmetric, is responsible for the behavior of the narrow lines. They report that "these lines are formed in a rapidly expanding region of the stellar wind which has a higher density than the ambient "quiet" wind and which has resulted from an enhanced mass flux of the star during a short time". Finally, they suggest that the appearance and variability of the high-velocity narrow absorption components are general properties of Be and other stars of early type and thus is a typical phenomenon for most OB stars.

Sadakane (1984) studied the spectra of the B star 36 Lyn and proposed that the SiIV and CIV resonance lines are formed in the hot outer atmosphere (chromosphere or corona)

Codina et al. (1984) suggested that as the resonance doublets of SiIV and CIV are asymmetric with extended blue wings, they probably indicate a tenuous expanding envelope. For the narrow absorption lines (SACs) of high ionized species such as SiIV, CIV and NV, they proposed that "they could originate in matter ejected occasionally by the star due to some kind of photospheric activity. In this line of thought, such an ejection is probably a localized phenomenon not associated with the whole surface of the star (blob)". Concerning the "blobs", they proposed that the gas inside them is probably hot, not necessarily in ionization equilibrium and that the ionization is caused by collisional processes.

Hubeny et al. (1985, 1986), found that the SiIV lines can be observed over the whole B spectral range. However, the "narrow components are observed only in B2 and earlier stars' spectra, indicate strongly mass outflows and large velocity fields in

early B stars, but they are not indicators of superionization. They suggested that “it will be possible to explain the observed UV spectra of at least some Be stars as a superposition of the contributions from the stellar atmosphere, the variable subionized Be envelope, and in some cases also from the (still unknown) medium producing the narrow blue-shifted components of resonance lines and/or from a transition zone in the accretion disk in interacting binaries”.

Danezis (1984, 1986) and Danezis et al. (1991) studied the UV spectra of the gaseous envelope of AX Mon taken by the IUE satellite and noted that the absorption lines of many ionization potential ions (including SiIV), not only of those presenting P Cygni profile, are accompanied by two strong absorption components of the same ion and the same wavelength, shifted at different  $\Delta\lambda$ , in the violet side of each main spectral line. This means that the regions where these spectral lines are created are not continuous, but they are formed by a number of independent density layers of matter. These layers of matter can rotate and move with different apparent velocities of the order of 10 km/s, -75 km/s and -260 km/s.

The existence of satellite components in the UV spectrum of AX Mon has been detected also by Sahade et al. (1984) and Sahade & Brandi (1985). For the SiIV absorption components, they found velocities between the values of -200 and +120 km/s. Also, Hutsemekers (1985), in the UV spectrum of another Be star, HD 50138, noticed a number of satellite components that accompanied the main spectral lines.

Aydin et al. (1988) studied the UV spectra of the binary system  $\beta$  Lyr and proposed that the profiles of SiIV resonance lines are formed by the superposition of a stationary P Cygni profile indicating the velocity of  $-162\pm 2$  km/s and a broad, less strong, symmetric emission, shifting back and forth through the orbital cycle. Such a result indicates that in the system “there are, at least, two high temperature regions, one close to the “unknown” companion to the B8II component and another one in the circumbinary region”. Finally, they observed some very sharp, undisplaced features (Hack et al., 1983) and they suggest that if some of them are created in the circumbinary envelope, they could indicate that, at a certain distance, the stellar wind in the system decelerates and when it merges with the interstellar medium, the velocities in both media have the same value.

Doazan et al. (1988) found that in the UV spectra of the B8Ve star HD 23862 the SiIV resonance lines are not detectable during the epoch of strong shell, while, when the shell spectrum vanishes, they are unambiguously identified, shifted at  $-52\pm 4$  km/s. They argue with Hubeny et al. (1985) on the point that these superionized lines are produced by spurious effects due to blending of shell lines. They proposed that these superionized lines are always present, but difficult/impossible to detect, due to the shell lines.

Sapar & Sapar (1992) studied the UV spectra of  $\eta$  CMa and found that the SiIV resonance lines show changes in their profiles, suggesting the presence of some shell condensations moving with time-dependent radial velocities. They observed “blue-shifted satellite components belonging to expanding shell condensations”, with radial velocities -360 km/s, -180 km/s, -110 km/s and -30 km/s. They attributed the presence of strong unshifted resonance line components of SiIV to a hot circumstellar gas cloud. They concluded to such behavior being the result of “an extended expanding envelope having dense shells which move away from the star and have different velocities”.

Kempner & Richards (1999) studied the UV spectra of the binary system U Sag, which consists of a B8V primary and a G4IV secondary component. They proposed the existence of circumstellar material, as the SiIV resonance lines presented

an orbital variation in the shape of the asymmetric profiles and in the wavelength of the lines' center. However, as the SiIV lines' profile is almost stable in time, the structure of the circumstellar gas contributing to the ultraviolet emission must also be stable in time.

Finally, Danezis et al. (2002) attributed many of the peculiarities occurring in the spectra of Oe and Be stars to the existence of Satellite Absorption Components (SACs). In order to study all the lines presenting SACs, they proposed a model for the structure of the regions where the spectral lines that present SACs are created (Danezis et al., 2002, 2003).

In this paper we present the proposed by Danezis et al. (2003) line function of and we apply it to 42 BeV stars, in order to calculate the apparent rotation and expansion/contraction velocities and an expression of the optical depth ( $\xi$ ) of the density regions where the UV SiIV resonance lines are created.

## The model: Mathematical expression

Considering an area of gas consisting of  $i$  independent absorbing shells followed by a shell that both absorbs and emits and an outer shell of general absorption, we conclude to the function:

$$I_{\lambda} = \left[ I_{\lambda 0} \prod_i \exp\{-L_i \xi_i\} + S_{\lambda e} (1 - \exp\{-L_e \xi_e\}) \right] \exp\{-L_g \xi_g\}$$

where:  $I_{\lambda 0}$ : the initial radiation intensity,

$L_i$ ,  $L_e$ ,  $L_g$ : are the distribution functions of the absorption coefficients  $k_{\lambda i}$ ,  $k_{\lambda e}$ ,  $k_{\lambda g}$  respectively. Each  $L$  depends on the values of the apparent rotation velocity as well as of the radial expansion/contraction velocity of the density shell, which forms the spectral line ( $V_{rot}$ ,  $V_{exp}$ ),

$\xi = \int_0^s \Omega \rho ds$  is an expression of the optical depth  $\tau$ , where  $\Omega$ : an expression of

$k_{\lambda}$  and has the same units as  $k_{\lambda}$ ,

$S_{\lambda e}$ : the source function, which, at the moment when the spectrum is taken, is constant and

$$L = \sqrt{1 - \cos^2 \theta_0} \text{ if } \cos \theta_0 < 1 \text{ and } L = 0 \text{ if } \cos \theta_0 \geq 1,$$

where  $\cos \theta_0 = \frac{-\lambda_0 + \sqrt{\lambda_0^2 + 4\Delta\lambda^2}}{2\Delta\lambda z_0}$ , where  $2\theta_0$  is the angular width of the

equatorial disk of matter,  $\lambda_0$  is the wavelength of the center of the spectral line and  $\lambda_0 = \lambda_{lab} + \Delta\lambda_{exp}$ , with  $\lambda_{lab}$  being the laboratory wavelength of the spectral line produced by a particular ion and  $\Delta\lambda_{exp}$  the radial Doppler shift and

$$\frac{\Delta\lambda_{exp}}{\lambda_{lab}} = \frac{V_{exp}}{c}.$$

$z_0 = \frac{V_{rot}}{c}$ , where  $V_{rot}$  is the apparent rotation velocity of the  $i$  density shell of matter and

$\Delta\lambda = |\lambda_i - \lambda_0|$ , where the values of  $\lambda_i$  are taken in the wavelength range we want to reproduce.

The spectral line's profile, which is formed by the  $i$  density shell of matter, must be accurately reproduced by the function  $e^{-L_i \xi_i}$  by applying the appropriate values of  $V_{\text{rot}i}$ ,  $V_{\text{exp}i}$  and  $\xi_i$ . Using the best model's fit for a complex spectral line, we can calculate the apparent expansion/contraction ( $V_{\text{exp}i}$ ) velocity, the apparent rotation velocity ( $V_{\text{rot}i}$ ) and an expression of the optical depth ( $\xi_i$ ) of the region in which the main spectral line and its SACs are created.

The depth of the absorption lines, which arise from the proposed model, depends only on  $\xi$ , while the height of the emission does not depend only on  $\xi_e$ , but on  $S_{\lambda_e}$  as well. For this reason, we name  $S_{\lambda_e} \xi_e$  height of the emission and we use it in the case of the emission, in the same way as we use  $\xi$  in the case of the absorption. The equation  $S_{\lambda_e} \xi_e = \int_0^s \Omega_e \rho_e ds$ , which corresponds to the emission, has the same form as the equation  $\xi = \int_0^s \Omega \rho ds$ , which corresponds to the absorption.

At this point we would like to point out that the calculated values of the apparent rotation and expansion/contraction velocities correspond to the regions, where the Satellite Absorption Components (SACs) are created, and not to the star. Specifically, these values correspond to the density regions (blobs, puffs, bubbles) which result when streams of matter are twisted and form strings that produce blobs, puffs or bubbles.

## Data

The data we used are the SiIV resonance lines of 42 Be V stars. The stars' spectrograms have been taken with IUE satellite and their spectral types have been taken by the SIMBAD database (Centre de Donnees Astronomiques de Strasbourg (CDS), Strasbourg, France). Our data are presented in table 1.

Table 1					
Star	Spectral Type	Camera	Star	Spectral Type	Camera
HD 206773	B0 V : pe	Swp 18753	HD 32343	B2.5 V e	Swp 06932
HD 200310	B1 V e	Swp 10853	HD 37967	B2.5 V e	Swp 21491
HD 212571	B1 V e	Swp 07009	HD 65875	B2.5 V e	Swp 06544
HD 35439	B1 V pe	Swp 07716	HD 187811	B2.5 V e	Swp 19937
HD 44458	B1 V pe	Swp 18306	HD 191610	B2.5 V e	Swp 08600
HD 200120	B1.5 V nne	Swp 09458	HD 208682	B2.5 V e	Swp 19935
HD 30076	B2 V e	Swp 20844	HD 20336	B2.5 V ne	Swp 19934
HD 32991	B2 V e	Swp 14840	HD 60855	B2/B3 V	Swp 21915
HD 50083	B2 V e	Swp 15958	HD 51354	B3 ne	Swp 16547
HD 58050	B2 V e	Swp 16536	HD 25940	B3 V e	Swp 07011
HD 164284	B2 V e	Swp 08614	HD 45725	B3 V e	Swp 28106
HD 41335	B2 V ne	Swp 08604	HD 183362	B3 V e	Swp 31218
HD 52721	B2 V ne	Swp 25377	HD 208057	B3 V e	Swp 05909
HD 58343	B2 V ne	Swp 08605	HD 205637	B3 V : p	Swp 07008
HD 148184	B2 V ne	Swp 07753	HD 217543	B3 V pe	Swp 31186
HD 194335	B2 V ne	Swp 19938	HD 22192	B5 V e	Swp 08593
HD 202904	B2 V ne	Swp 08601	HD 138749	B6 V nne	Swp 09124
HD 65079	B2 V ne...	Swp 53980	HD 192044	B7 V e	Swp 28251
HD 28497	B2 V : ne	Swp 08594	HD 22780	B7 V ne	Swp 20846
HD 45995	B2 V nne	Swp 09936	HD 18552	B8 V ne	Swp 55906
HD 10516	B2 V pe	Swp 08592	HD 199218	B8 V nne	Swp 30071

## Spectral analysis of the SiIV resonance lines in the UV spectra of 42 Be V stars

### Figures

In figures 1 and 2 we present the SiIV lines' fittings of 10 BeV stars together with the normal B star's HD 30836 SiIV profile, in order to indicate the blended lines and the intense appearance of the SACs. The thick line presents the observed spectral line's profile and the thin one the model's fit. The dashed lines indicate the laboratory wavelengths of the SiIV resonance lines at  $\lambda\lambda$  1393.755, 1402.77 Å.

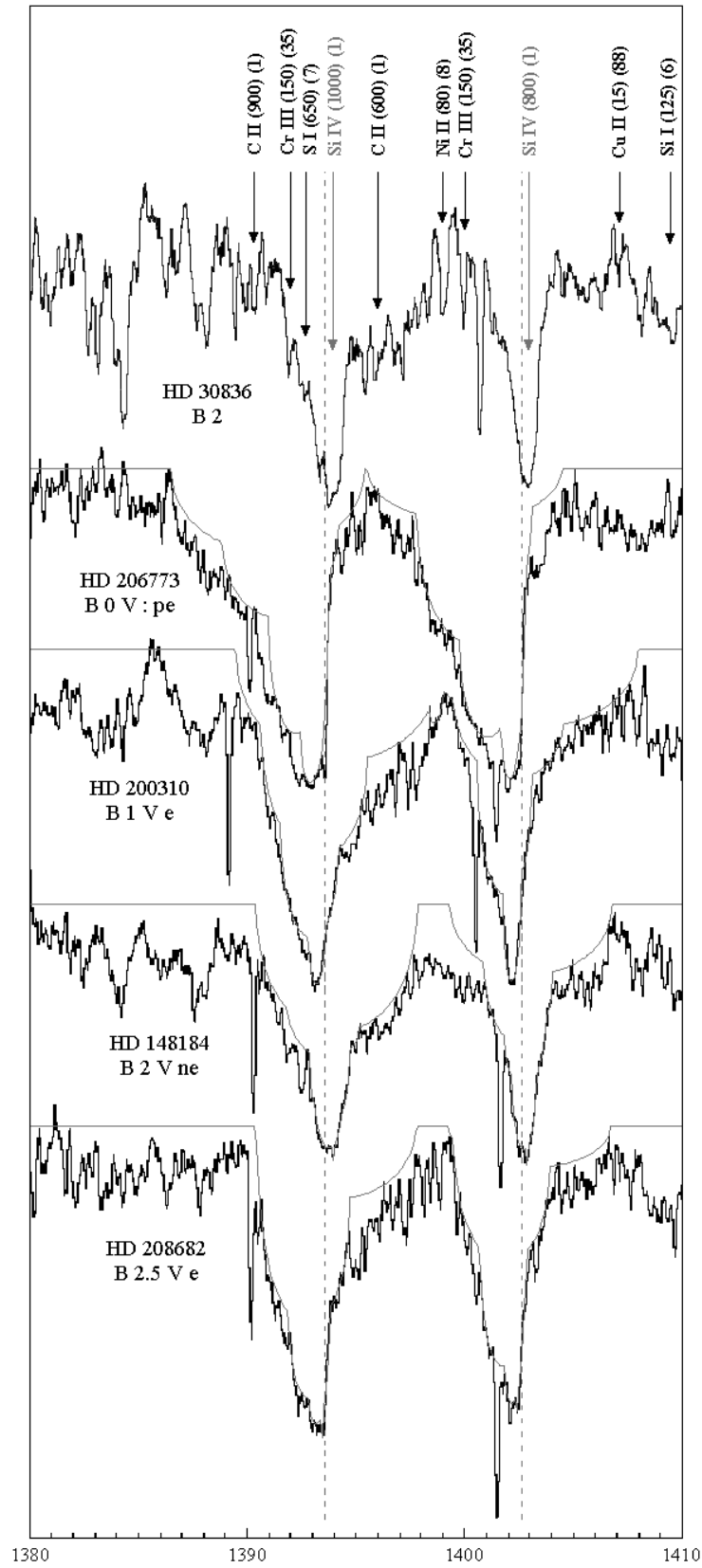


Figure 1

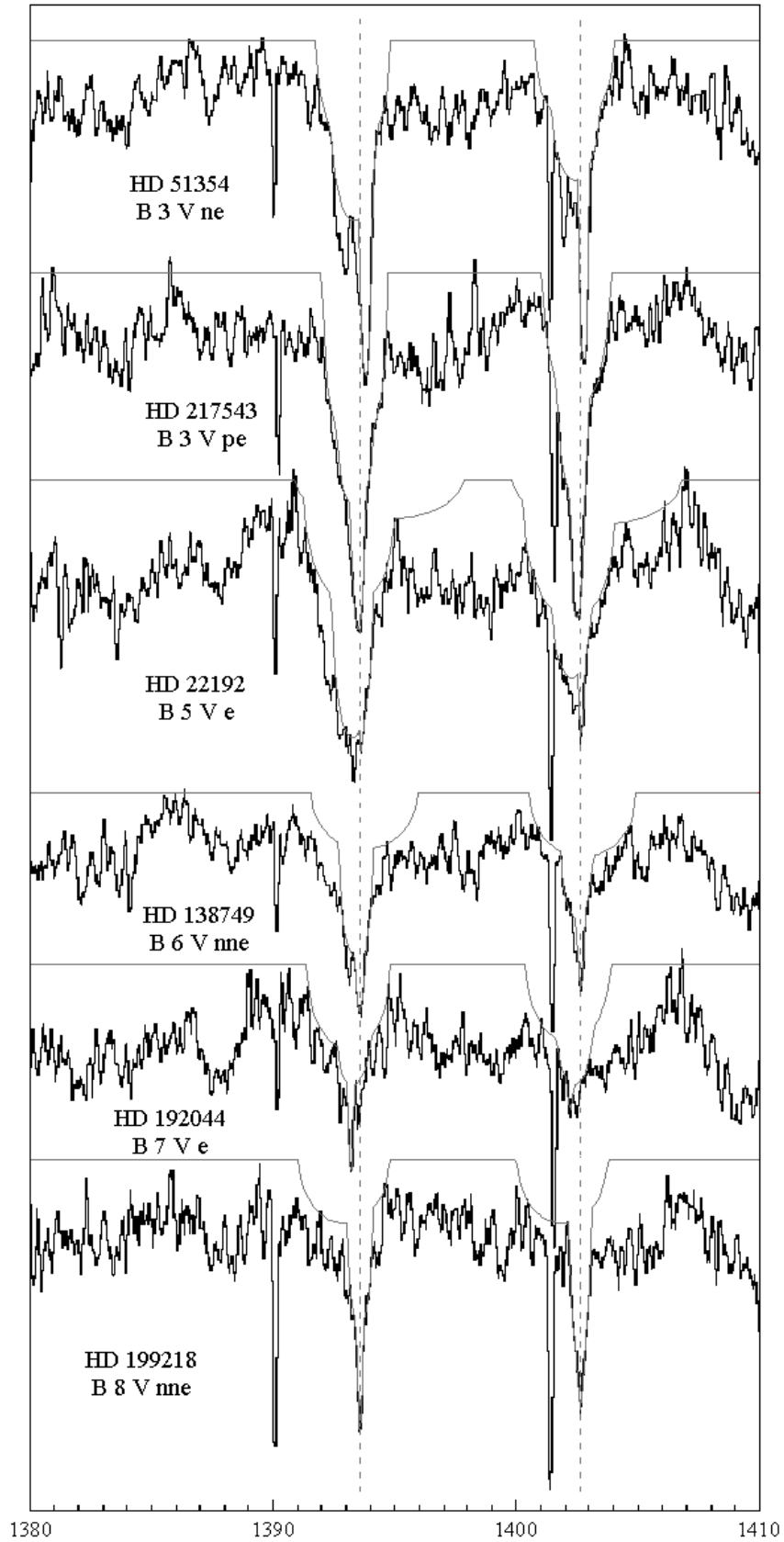
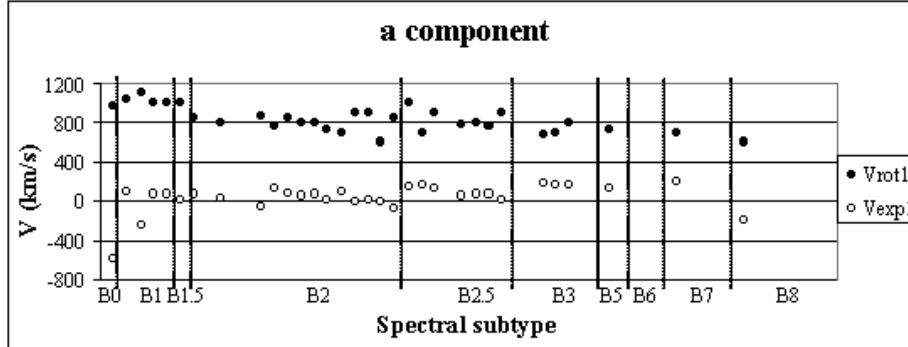
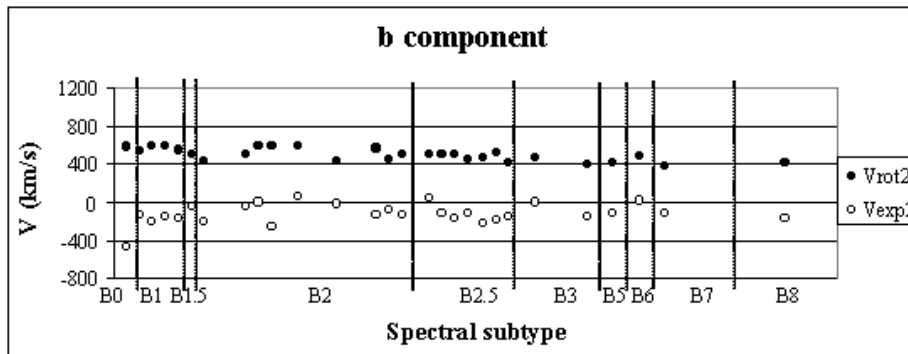


Figure 2

## Diagrams and Conclusions



**Diagram 1:** Apparent rotation and expansion/contraction velocities of the first SAC as a function of the spectral subtype. As one can see, the first SAC's rotation and expansion/contraction velocities present a uniform fluctuation around the values of 830 km/s and +31 km/s respectively.



**Diagram 2:** Apparent rotation and expansion/contraction velocities of the second SAC as a function of the spectral subtype. A uniform fluctuation is also presented in the second SAC's rotation and expansion/contraction velocities around the values of 492 km/s and -131 km/s respectively.

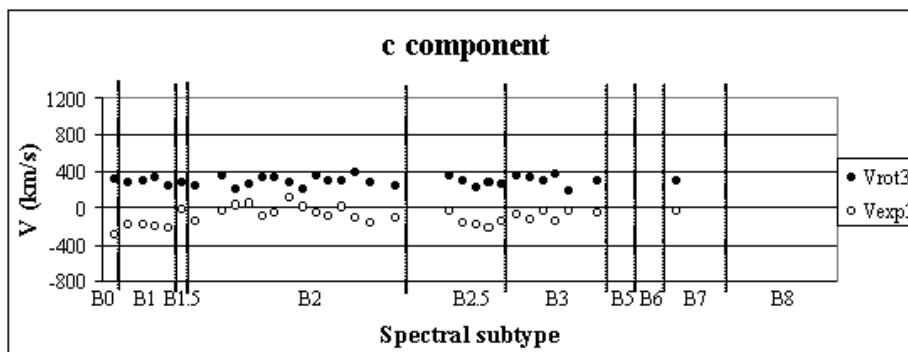


**Diagram 3:** Apparent rotation and expansion/contraction velocities of the third SAC as a function of the spectral subtype. The third SAC's rotation and expansion/contraction velocities fluctuate around the values of 285 km/s and -105 km/s respectively.

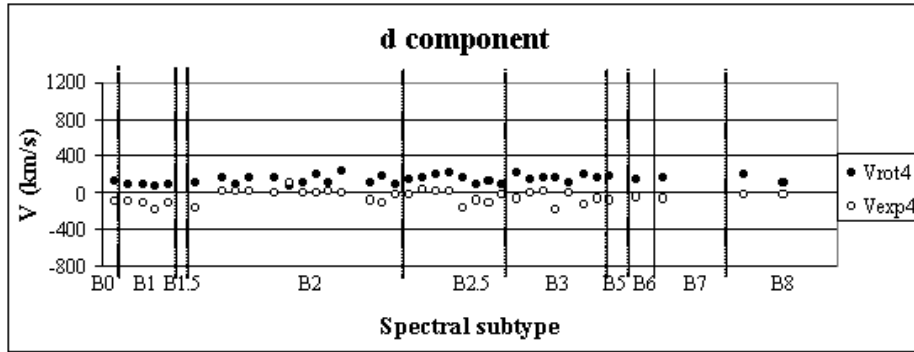


**Diagram 4:** Apparent rotation and expansion/contraction velocities of the fourth SAC as a function of the spectral subtype. The fourth SAC's rotation and expansion/contraction velocities fluctuate around the values of 137 km/s and -54 km/s respectively.

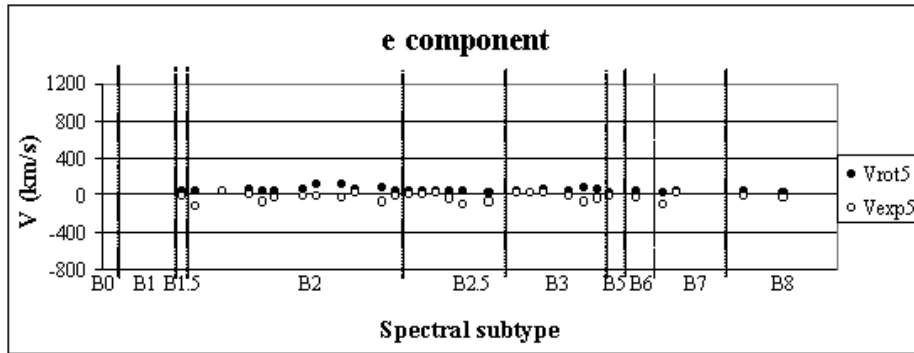


**Diagram 5:** Apparent rotation and expansion/contraction velocities of the fifth SAC as a function of the spectral subtype. The fifth SAC's rotation and expansion/contraction velocities fluctuate around the values of 51 km/s and -25 km/s respectively.

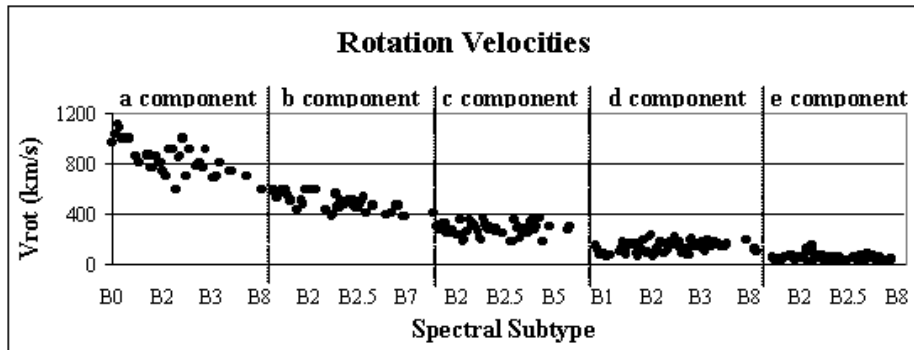


**Diagram 6:** Apparent rotation velocities of all the SACs as a function of the spectral subtype (presented separately). Five levels of rotation velocity are presented with the mean values of 830 km/s, 492 km/s, 285 km/s, 137 km/s and 51 km/s.

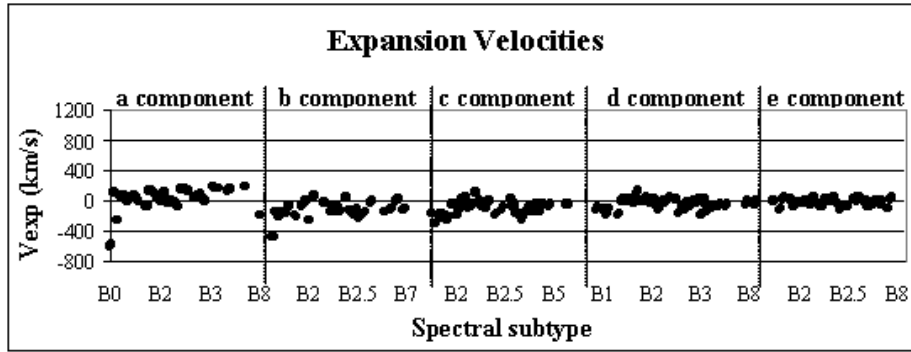


**Diagram 7:** Apparent expansion/contraction velocities of all the SACs as a function of the spectral subtype (presented separately). The values of the expansion/contraction velocity of all the SACs lie in the range between -306 km/s and +194 km/s.

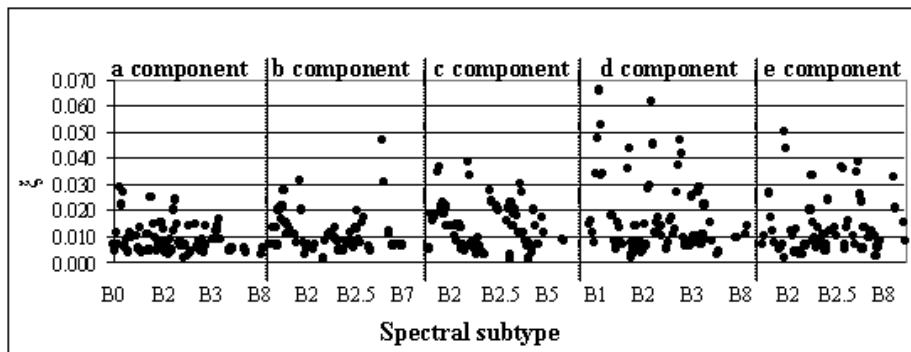


**Diagram 8:** The  $\xi$  values of each SAC as a function of the spectral subtype. For the first SAC the values of  $\xi$  lie between 0.002 and 0.029, while for the second SAC and the third SAC the values of  $\xi$  lie mainly in the range, between 0.001 and 0.039. For the fourth and the fifth SAC the values of  $\xi$  present great dispersion and lie, mainly, in the range between 0.002 and 0.052.

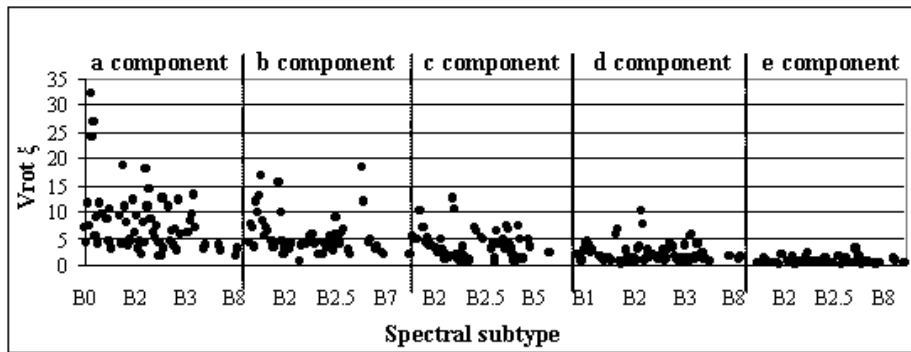


**Diagram 9:** Values of the product of  $\xi$  and the apparent rotation velocities ( $V_{rot}\xi$ ) as a function of the spectral subtype, presented separately for each SAC. The product  $V_{rot}\xi$  is an expression of the absorbed energy.

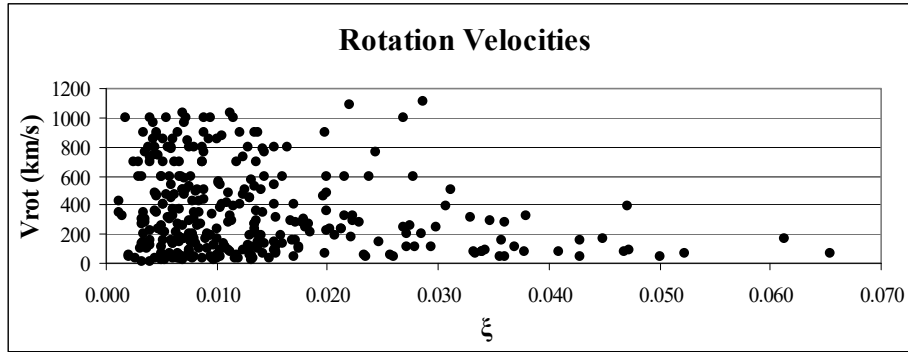


**Diagram 10:** Apparent rotation velocities of all the SACs as a function of the respective value of  $\xi$ . For small values of  $\xi$  (0.001-0.029) the rotation velocity lies in the range of 12 to 1110 km/s. As the value of  $\xi$  increases (0.030-0.065) the rotation velocity's values lie in a smaller range between 40 and 500 km/s. It is apparent that most of the SACs present small values of  $\xi$ . The points with greater values of  $\xi$  correspond to the fourth and fifth SACs, as one can see in diagram 8.

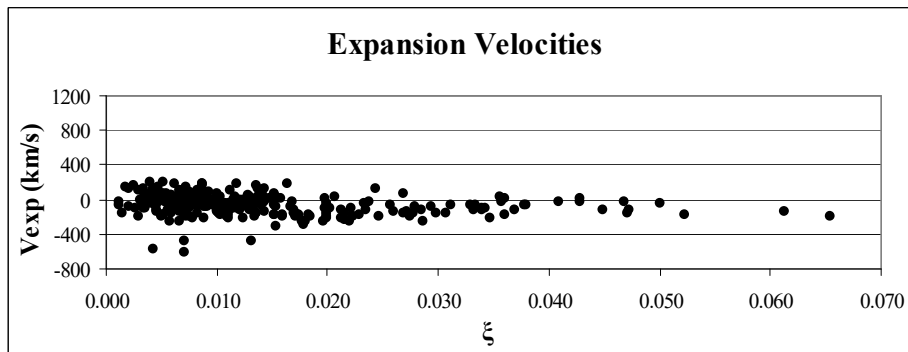


**Diagram 11:** Expansion/contraction velocities of all the SACs as a function of the respective value of  $\xi$ . For small values of  $\xi$  (0.001-0.029) the expansion/contraction velocity lies, mainly, in the range of -306 to +194 km/s. As the value of  $\xi$  increases the expansion/contraction velocity's values lie in a smaller range between -222 and +21 km/s.

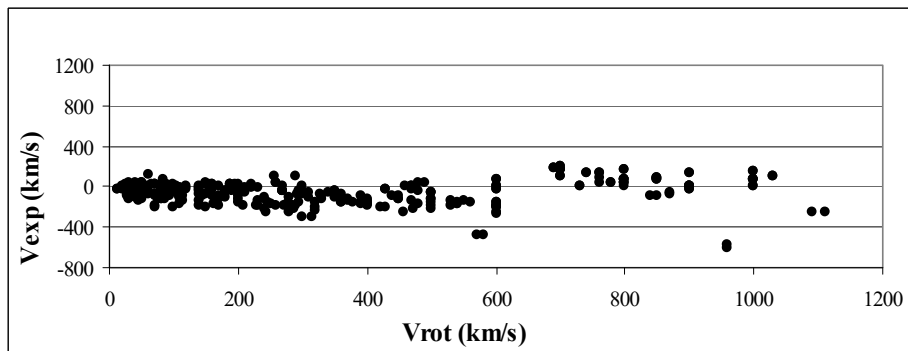


**Diagram 12:** Expansion/contraction velocities of all the SACs as a function of the respective apparent rotation velocities. For the smaller values of the rotation velocity (12 - 560 km/s) the values of the expansion/contraction velocity lie in a small range between -306 and +118 km/s. As the rotation velocity increases (570 and 1110 km/s) the expansion/contraction velocity presents greater dispersion and lies between -608 and +192 km/s.

## References

- Aydin, C., Brandi, E., Engin, S., Ferrer, O. E., Hack, M., Sagade, J., Solivella, G. & Yilmaz, N.: 1988, *A&A*, 193, 202
- Bruhweiler, F. C., Grady, C. A. & Chiu, W. A.: 1989, *ApJ*, 340, 1038
- Codina, S. J., de Freitas Pacheco, J. A., Lopes, D. F. & Gilra, D.: 1984, *A&AS*, 57, 239
- Danezis, E.: 1984, The nature of Be stars, PhD Thesis, University of Athens.
- Danezis, E.: 1986, IAU, Colloq. No 92, Physics of Be Stars, Cambridge University Press.
- Danezis, E., Theodossiou, E. & Laskarides, P.G.: 1991, *Ap&SS*, 179, 111-139.
- Danezis, E., Nikolaidis, D., Lyratzi, E., Stathopoulou, M., Theodossiou, E., Kosionidis, A., Drakopoulos, C., Christou, G. & Koutsouris, P.: 2002, A new model of density layers of matter in the expanding gaseous envelope of Oe and Be stars. Proceedings of the IAU Symposium 210: Modeling of stellar atmospheres, June 17 21, 2002, Uppsala, Sweden.
- Danezis, E., Nikolaidis, D., Lyratzi, V., Stathopoulou, M., Theodossiou, E., Kosionidis, A., Drakopoulos, C., Christou G. & Koutsouris, P.: 2003, *Ap&SS*, 284, 1119
- Doazan, V., Thomas, R. N. & Bourdonneau, B.: 1988, *A&A*, 205L, 11
- Gathier, R., Lamers, H. J. G. L. M. & Snow, T. P.: 1981, *ApJ*, 247, 173
- Hack, M., Sahade, J., de Jager, C. & Kondo, Y.: 1983, *A&A*, 126, 115
- Henize, K. G., Wray, J. D., Parsons, S. B. & Benedict, G. F.: 1976, *IAUS*, 70, 191
- Henize, K. G., Wray, J. D. & Parsons, S. B.: 1981, *AJ*, 86, 1658
- Henrichs, H. F., Hammerschlag-Hensberge, G., Howarth, I. D. & Barr, P.: 1983, *ApJ*, 268, 807
- Hubeny, I., Stefl, S. & Harmanec, P.: 1985, *BAICz*, 36, 214
- Hubeny, I., Harmanec, P. & Stefl, S.: 1986, *BAICz*, 37, 370
- Hutsemekers, D.: 1985, *A&AS*, 60, 373-388.
- Israelian, G.: 1995, *A&A*, 300, 834
- Kempner, J. C. & Richards, M. T.: 1999, *ApJ*, 512, 345
- Kondo, Y., McCluskey, G. E. & Harvel, C. A.: 1981, *ApJ*, 247, 202
- Lamers, H. J. G. L. M. & Snow, T. P.: 1978, *ApJ*, 219, 504
- Marlborough, J. M.: 1982, *IAUS*, 98, 361
- Marlborough, J. M. & Peters, G. J.: 1982, *IAUS*, 98, 387
- Panek, R. J. & Savage, B. D.: 1976, *ApJ*, 206, 167
- Plavec, M. J.: 1983, *ApJ*, 275, 251
- Prinja, R. K.: 1990, *MNRAS*, 246, 392
- Sadakane, K.: 1984, *PASP*, 96, 259
- Sahade, J., Brandi, E. & Fontela, J.M.: 1984, *A&AS*, 56, 17.
- Sahade, J. & Brandi, E.: 1985, *Rev. Mex.*, 10, 229.
- Sapar, L. & Sapar, A.: 1992, *BaltA*, 1, 37
- Snow, T. P. & Marlborough, J. M.: 1976, *ApJ*, 230L, 87
- Snow, T. P. & Morton, D. C.: 1976, *ApJS*, 32, 429
- Snow, T. P.: 1977, *ApJ*, 217, 760
- Underhill, A. B.: 1974, *ApJS*, 27, 359
- Underhill, A. B.: 1975, *ApJ*, 199, 691
- Walborn, N. R. & Nichols-Bohlin, J.: 1987, *PASP*, 99, 40